Journal of The Electrochemical Society, **157** (4) C140-C145 (2010)
0013-4651/2010/157(4)/C140/6/$28.00 © The Electrochemical Society

Anodic Electrodeposition of Germanium Films from Ethylenediamine Solutions of Deltahedral Ge_9^{4-} Zintl Ions

Nirmala Chandrasekharan and Slavi C. Sevov[z]

Department of Chemistry and Biochemistry, University of Notre Dame, Notre Dame, Indiana 46656, USA

In this work, we report studies of germanium electrodeposits galvanostatically electroplated anodically onto p-doped Si(100) wafers for three different current densities under ambient conditions. The electrodeposition is carried out in ethylenediamine solutions of K_4Ge_9, which contain deltahedral Ge_9^{n-} (n = 2, 3, 4) Zintl anions. The observed current efficiencies of the deposition are at least 2 orders of magnitude higher than those of cathodic electroplating reported. The samples were characterized by scanning electron microscopy (SEM), energy-dispersive X-ray analysis, X-ray photoemission spectroscopy, and mass spectrometry. Their morphology is sheetlike with overlayers of aggregated particles with a median particle size of ~225 nm. The overlayer spread increases progressively with increasing current densities. Cross-sectional SEM measurements indicate film thicknesses in the range of 60–320 nm. Electrolytic electrodeposition carried out at 100 V for the same concentration reveals a very similar morphology with significant enhancement in thickness of up to ~6 μm and median particle size of 625 nm. X-ray diffraction shows that the as-deposited samples are amorphous; however, high temperature annealing results in the crystallization of elemental germanium in the thicker samples (~320 nm and ~6 μm).
 [DOI: 10.1149/1.3309726]

Manuscript submitted August 7, 2009; revised manuscript received January 12, 2010. Published March 10, 2010.

Amorphous and crystalline films of group IV semiconductors such as Ge are of great interest, owing to their applications in novel optoelectronic as well as energy conversion devices.[1] There are several well-established techniques devoted to their fabrication, including chemical vapor deposition,[2] electron-beam evaporation,[3] pulsed laser deposition,[4] ion implantation,[5] molecular beam epitaxy,[6] and sputtering.[7] All these techniques require vacuum or ultrahigh vacuum for deposition. In this regard, electrochemical deposition is a comparatively simple, one-step, and cost-effective method. It is advantageous in several respects. For instance, the structure, surface morphology, and uniformity of the deposits can be easily controlled by adjusting the parameters of electrochemical deposition such as the deposition mode, applied potential, current density, bath temperature, concentration of precursors, and addition of complex/additive agents.[8] Reports related to electrodeposition of Ge films[9] on metallic and semiconductor substrates are very few.[10] The reason is that due to the low overpotential of hydrogen on germanium surfaces in aqueous solutions, once a very limited amount of Ge is deposited on the electrode surface, all the plating current subsequently is used for proton reduction.[11] In approaches wherein nonaqueous solutions are used, e.g., propylene glycol or ionic liquids, there are disadvantages related to the need for high temperatures and high current densities or high costs. This is why there are so few papers about electrodeposition of germanium on silicon substrates. Mukhopadhyay and Freyland[12] electrodeposited ultrathin films of elemental Ge onto silicon substrates from a solution of $GeCl_4$ in the ionic liquid 1-butyl-3-methyl imidazolium hexafluorophosphate. A thickness-dependent metal to nonmetal transition has been observed for ultrathin films of electrodeposited Ge. Huang et al. demonstrated the growth of cathodically electroplated amorphous Ge thin films on $Si_3N_4/SiO_2/Si$ patterned substrates[13] as well as on blank n- and p-doped Si substrates[14] using a germanium tetrachloride solution in 1,3-propanediol at 60–80°C.

In the light of the scenario aforementioned, there is an ongoing effort to develop new cost-effective synthetic pathways for the fabrication of thin films of semiconductors that can exhibit improved efficiency and selectivity toward light energy conversion and semiconductor optoelectronics. In this context, the solid-state chemistry of Zintl phases with anionic fragments made of metallic or semiconducting p-elements is very rich and yet largely unexplored from the point of view of applications in solution media. There are a few papers that employ germanium-based Zintl phases to obtain solutions or suspensions for the preparation of nanoparticles. For example, suspensions of the Zintl phases NaGe, KGe, and Mg_2Ge in boiling glymes have been used in metathesis reactions with $GeCl_4$ or metal halides to produce halide-terminated germanium particles.[15,16] Similarly, hexagonal mesoporous germanium has been obtained by a slow oxidative polymerization of the deltahedral Ge_9^{4-} clusters in the presence of and mediated by the cationic surfactant *N*-eicosane-*N*,*N*-dimethyl-*N*-(2-hydroxyethyl)ammonium bromide.[17] In another paper, ethylenediamine solutions of K_4Ge_9 are treated with cetyltriethylammonium bromide and, according to low angle X-ray diffraction, the resulting precipitate has a hexagonal honeycomb structure with a well-defined nanometer scale order.[18] Similarly, composite thin films with hexagonal architectures have been prepared by treating solutions of the Zintl phase $K_4Ge_4Se_{10}$ with various transition-metal salts in the presence of templates such as cetyltriethylammonium bromide.[19]

There are only a few papers of anodically electrodeposited films of semiconducting or metallic elements,[20] and the obvious reason for this is the natural tendency for metals and semiconductors to form cationic rather than anionic species in solutions. Nonetheless, anions of main-group metals and semimetals exist, and these are the well-known Zintl ions stable in liquid ammonia or ethylenediamine solutions. One class of these is the nine-atom deltahedral cluster anions of group 14, namely, E_9^{4-} for E = Si, Ge, Sn, and Pb (Fig. 1), which can be extracted in solutions from Zintl phases that already contain them. Here, we report anodic electrodeposition of germanium films on p-doped Si(100) substrates from ethylenediamine solutions of such germanium Zintl ions, Ge_9^{4-}.

Experimental

Electrodeposition was carried out inside a nitrogen-filled glove box. Wafers of boron-doped Si(100) (MEMC Electronic Materials, Inc.) were cut into 4 × 0.8 cm strips, which were used as anodes. The strips were cleaned using the standard RCA process. Before electrolytic deposition, the substrates were further treated with 2% HF for 2 s, rinsed in ethanol and water, and vacuum-dried. Ohmic contacts between the strips and the terminal wires were achieved by coating the wires with InGa eutectic at the point of contact and then ensuring that the contact was secured by an additional coat of epoxy glue on top of the junction. The resistivities of these as-prepared electrodes were measured to be in the range of 150–200 kΩ cm. Copper wire was used as the counter electrode. The wires were connected to ports on the glove box that led to the external circuitry (outside the box). A cuvette of 1 cm width with a well-fitted Teflon lid with holes for the terminal wires of the two electrodes was used for electrodeposition. The constant-current electrodeposition was carried out with a PAR model 173 galvanostat in conjunction with a

[z] E-mail: ssevov@nd.edu

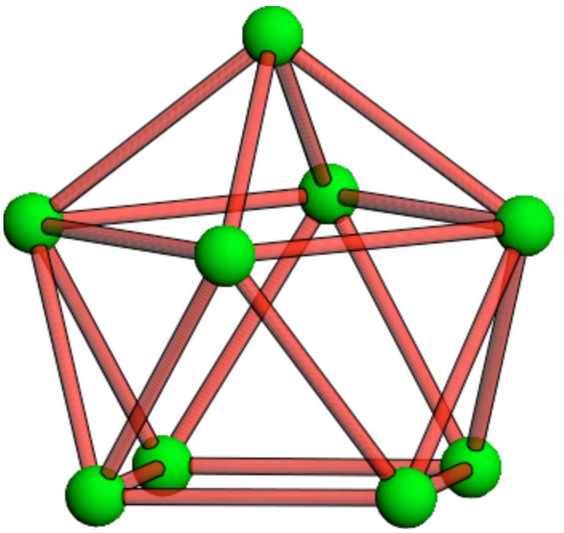

Figure 1. (Color online) A view of the nine-atom deltahedral Zintl ions E_9^{4-} (E = Si, Ge, Sn, Pb) with the shape of a monocapped square antiprism.

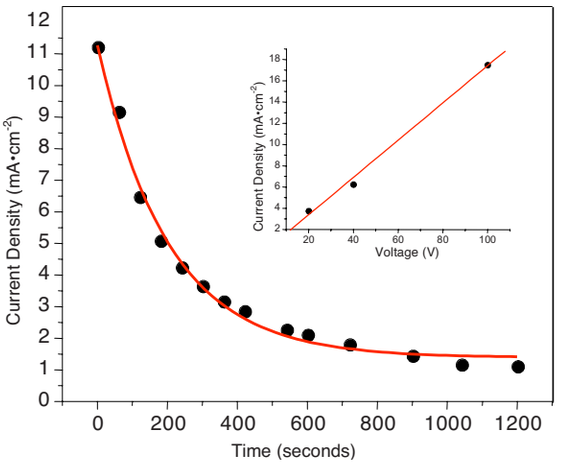

Figure 2. (Color online) Time dependence of the anodic current density in electrolytic deposition of germanium films from a 0.01 M solution of K_4Ge_9 in ethylenediamine at 100 V. The solid line represents the fitted exponential decay. The inset shows the linear increase in the current density with electric field strength for a 0.1 M solution.

model 176 current follower. A common multimeter and a power source (Harrison Inc., 6515A dc power supply) were used as well.

X-ray powder diffraction of the films was carried out on a Scintag X-1 diffractometer (λ = 1.5412 Å) in the 2θ range of 10–80°. Scanning electron microscopy (SEM) images and energy-dispersive spectroscopy (EDS) analysis were taken on a Hitachi S-4500 field-emission-scanning electron microscope equipped with a Hitachi Pulse Tor silicon drift detector. X-ray photoemission spectroscopy (XPS) measurements were conducted using a Kratos XSAM 800 instrument with a Mg Kα source (1253.6 eV). The C 1s peak was used as the internal standard.

The precursor compound with nominal composition K_4Ge_9 was synthesized according to the standard literature procedure.[21] Potassium and germanium metals were mixed together in stoichiometric amounts and heated to 900°C for 2 days in sealed (by arc-welding) niobium containers that were jacketed in evacuated fused-silica ampoules. Solutions were prepared by dissolving the precursor in ethylenediamine and by stirring it overnight. They were then centrifuged and filtered before use.

Results and Discussion

Our investigations started with testing for anodic electrodeposition in electrolytic mode with an input voltage of 100 V set by the power supply, and the depositions were carried out for 20 min from ethylenediamine solutions of the K_4Ge_9 precursor (0.01 or 0.10 M). The electrolysis produced adherent homogeneous grayish-violet and gray black films for the 0.01 M and 0.1 M electrolyte solutions respectively that were then further studied by measuring various aspects of the deposition. Thus, the current density was measured as a function of time of deposition as well as field strength (Fig. 2). The latter, measured for 0.1 M solutions, showed linear dependence, implying an ohmic conduction (Fig. 2 insert).

The time of deposition dependence fitted well to a first-order exponential decay with a time constant of 202(11) s (Fig. 2). The relatively high concentration of the electroactive species (Ge_9^{4-}) creates a very high initial anodic current at the onset of electrodeposition. The deposition of germanium starts once the electric double layer at the silicon surface is stabilized. The film growth depends on the number of electrochemical equivalents required to neutralize (oxidize) the electroactive species Ge_9^{n-}. The electrodeposition stops when either the electrical resistance of the growing film becomes sufficiently high to impede the passage of current through the film or the source of germanium is depleted. The latter is easily eliminated in our case because the concentrations of the clusters are so high that multiple sequential depositions can be carried out by inserting fresh and clean silicon anodes.

After these initial electrolytic depositions, we carried out more controlled experiments, namely, depositions at constant currents. Thus, films were deposited at three different current densities of 0.3, 1.3, and 3 mA/cm^2 with each deposition lasting for 1 min. Adherent bright and homogeneous but much thinner films were obtained in these cases.

One important parameter for electrodeposition is the current efficiencies of the depositions, i.e., the percentage of deposited material as a fraction of the theoretically calculated amount based on the used coulombs in the process. These numbers for the electrolytic deposition at 100 V and the constant-current deposition at 3 mA/cm^2 were quite high, at around 73 and 51%, respectively. (The amounts of germanium deposited at 0.3 and 1.3 mA/cm^2 were too small to accurately weigh.) In contrast, Huang et al.[13] reported only a 0.3% current efficiency for their cathodic electroplating of Ge on n-Si(100) and highly doped p-Si(111) substrates from $GeCl_4$ solution in 1,3-propanediol.[13] The authors attribute this low current efficiency to the enhanced hydrogen evolution on the Ge surface. In our work, the current efficiencies are 2 orders of magnitude higher, which is not surprising because, unlike the cathodic case, there are no or very limited side reactions at the anode to contend. (Some partial oxidation of the ethylenediamine solvent is possible but, for all practical purposes, is negligible.)

The morphologies of the as-deposited films were examined by SEM. The films were rinsed in ethylenediamine several times until the rinsing solutions became colorless and were evacuated overnight before the SEM studies. The micrographs showed sheetlike films with cracks and with overlayers of aggregated spherical particles (Fig. 3 and 4). The particles show wide size distributions with median particle sizes of 625 nm for the films deposited at 100 and around 225 nm for those deposited at 1.3 and 3 mA/cm^2. There were no discernible layers of particles on the films deposited at current densities of up to 0.3 mA/cm^2. One plausible explanation for the observed morphology is that, initially, germanium is electrodeposited as nano- and microspheres that are then annealed into sheets. The annealing is caused by local heating at the anode surface which, in turn, is a result of the resistance buildup during electrodeposition. The subsequent cooling when the process is turned off perhaps causes the cracking of the sheets as well as leaves unannealed nanoparticulate overlayers. A similar morphology of plates

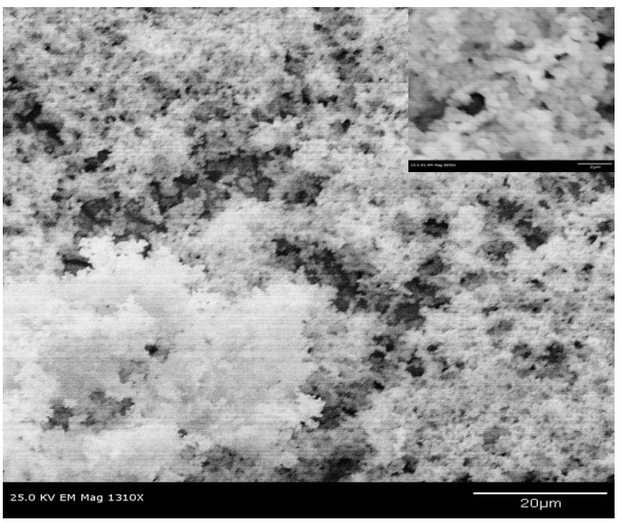

Figure 3. SEM micrograph of an electrodeposited germanium film showing sheetlike morphology with intermittent discernible cracks and aggregated spherical particles on top of the sheets (inset). The particles show a wide size distribution with a median particle size of 625 nm.

and overlayers of particles has been observed before for germanium films electrodeposited on Au(111) from GeX_4 (X = Br, I) dissolved in ionic liquids such as 1-butyl-3-methylimidazolium hexafluorophosphate.[22] The SEM images of such films deposited at a potential of −500 mV (vs bulk germanium) showed islandlike formations similarly covered with aggregated spherical particles. The authors commented that "in a wider sense, it (the film) is composed of coherent nanosized wires that seem to be built up of individual nanoclusters."

These nanosized wires, according to their observations, have grown from the surface of the electrode toward the solution.

Cross-sectional (thickness) measurements on the films were carried out on samples made by snapping the Ge-coated silicon wafers and imaging the exposed edges. The thickness of the samples deposited at 100 V was around 6 μm, whereas those deposited at constant currents had thicknesses between 60 and 320 nm. As expected for a "clean" process, the thickness is directly proportional to the charge density confirming that Faraday's law is obeyed (Fig. 5). A closer view of the cross section of the film deposited at 100 V is shown in Fig. 6. It exhibits well-defined platelets as well as the occurrence of an undulating continuous "bumpy" sheet with heights of the thickness order of the film. Saitou et al., in their paper on germanium thin films electrodeposited on copper substrates from a solution of $GeCl_4$ in propylene glycol, discussed at length the growth of such continuous mounds or bumps in the context of surface roughening in electrodeposited films.[23] According to the paper, the height fluctuations on the surfaces could be explained by statistical growth models. The scaling exponents that explain such a behavior are independent of the specific systems, insensitive to experimental conditions, and may depend on, for example, random fluctuations in the deposition process and/or surface tension. A review paper by Liu et al.[24] discusses at length the roughening of the surface due to induced strains, which, in turn, are the result of a lattice mismatch between film and substrate.

The compositions of the films were studied by EDS, laser desorption mass spectrometry, and XPS. A typical EDS spectrum is shown in Fig. 7. The peaks from the Ge Lα1, Kα1, and Kβ1 X-ray emissions are clearly seen along with the peak from the Si substrate. The peak due to O is small, ca. 1% of the Ge signal. Hence, one can conclude that oxidation of the Ge film, if it occurs at all, should be small and most likely occurs only on the surface.

The laser desorption time-of-flight mass spectrometry (in negative-ion mode) showed similar results. The samples were prepared by scraping small portions of the film, suspending the pow-

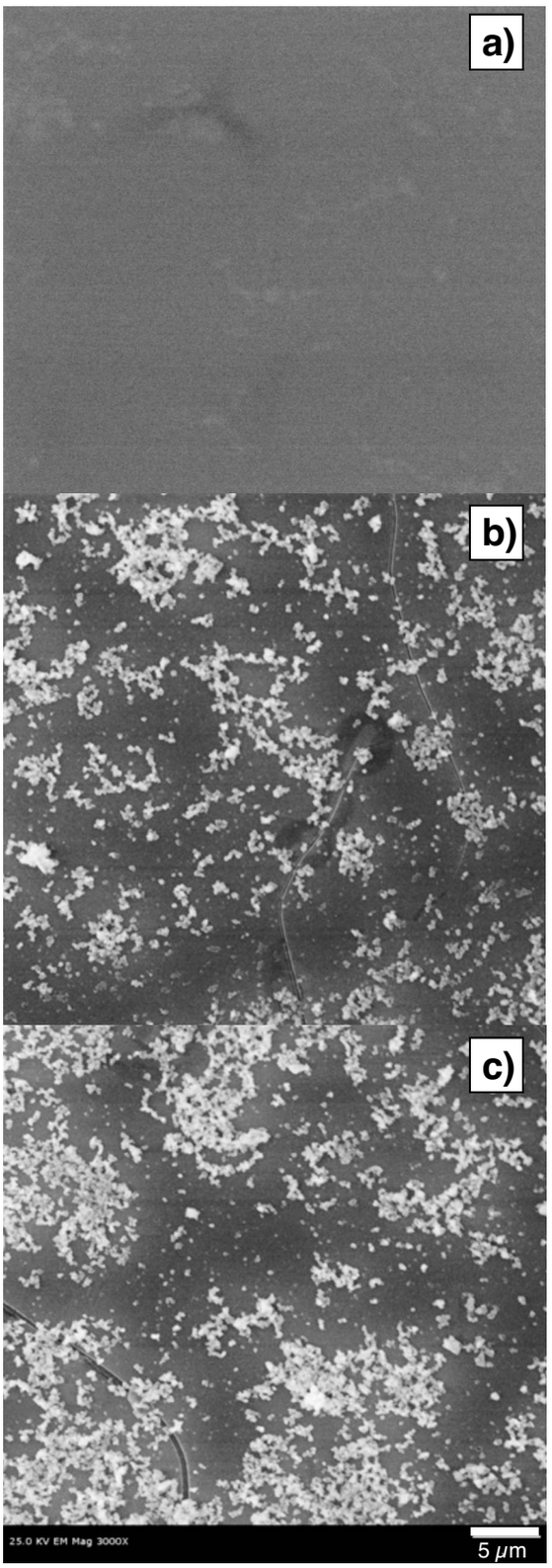

Figure 4. SEM micrographs of films deposited at constant-current densities of (a) 0.3, (b) 1.3, and (c) 3 mA/cm^2. Clearly, the film morphology remains the same above 1.3 mA/cm^2.

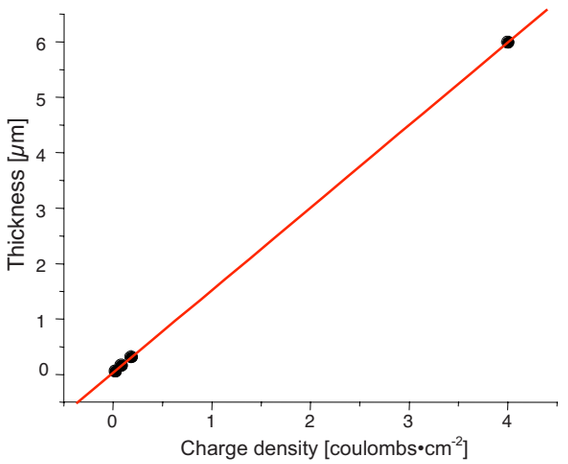

Figure 5. (Color online) Linear increase in germanium film thickness with charge density, confirming that the process follows Faraday's law.

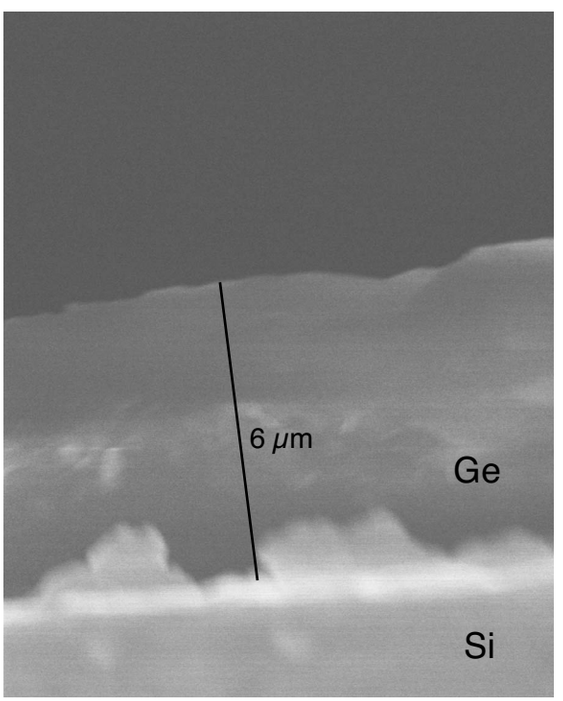

Figure 6. A cross-sectional SEM view of the germanium film on a silicon substrate. The maximum thickness is about 6 μm.

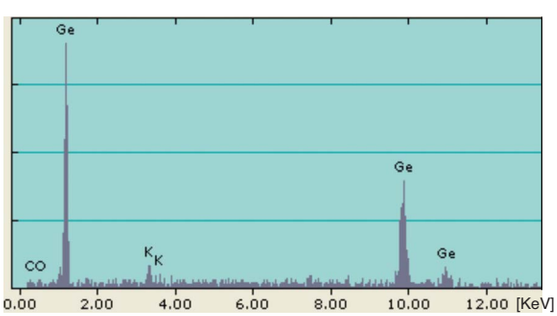

Figure 7. (Color online) An EDS spectrum of the electrodeposited germanium film on p-doped Si(100).

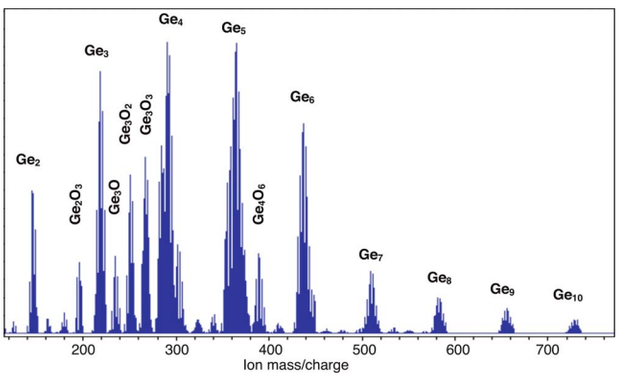

Figure 8. (Color online) A laser desorption mass spectrum of a germanium film electrodeposited on p-doped Si(100) surface.

dery material in dry acetonitrile, and placing small drops of the suspension on a conductive glass plate. The spectra (Fig. 8) showed anionic germanium clusters ranging from 2 to 10 atoms (ratio of mass to charge, m/z values of 146, 219, 291, 365, 437, 509, 582, 655, and 725) with abundances that decreased with increasing cluster size. Several peaks corresponding to germanium oxides ($Ge_2O_3^-$, Ge_3O^-, $Ge_3O_2^-$, $Ge_3O_3^-$) are also present. The spectra are remarkably similar to those reported by Fässler and co-workers in their laser desorption studies on mixtures of elemental K and Ge.[25] They observed exactly the same cluster sizes and the same traces of germanium oxides. The presence of oxides, in our case, is most likely due to oxidation of small amounts of negatively charged germanium species in the form of clusters or in intermetallics counterbalanced by potassium cations, i.e., K_xGe_y, on the surface of the films. This is corroborated by the observed traces of potassium in the EDS spectra as well as by the observed surface oxidation and traces of potassium in the XPS spectra (Fig. 9). The spectra of the as-prepared films, i.e., without surface "cleaning," showed only oxidized germanium. However, after the removal of a couple of surface monolayers by sputtering with Ar^+ ions for 10 min (removes a layer

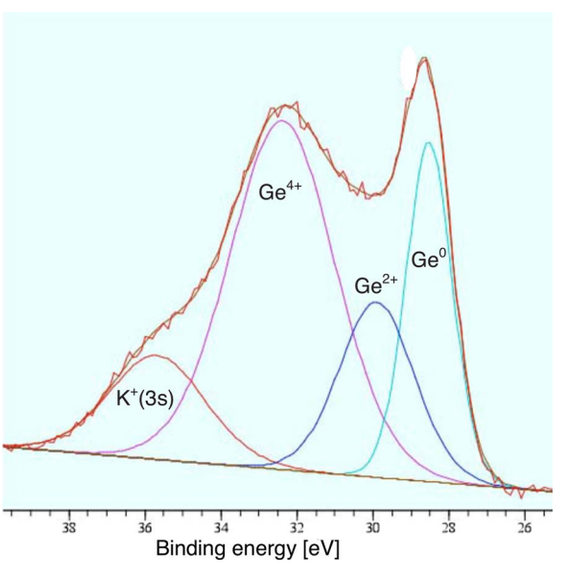

Figure 9. (Color online) A segment of the XPS spectrum of the germanium film after removal of a couple of surface monolayers by sputtering with Ar^+. The deconvolution of the spectrum shows the presence of 3d electrons of both oxidized (Ge^{4+},Ge^{2+}) and elemental germanium. The K^+ 3s electrons are most likely from potassium oxides captured in the cracks of the film.

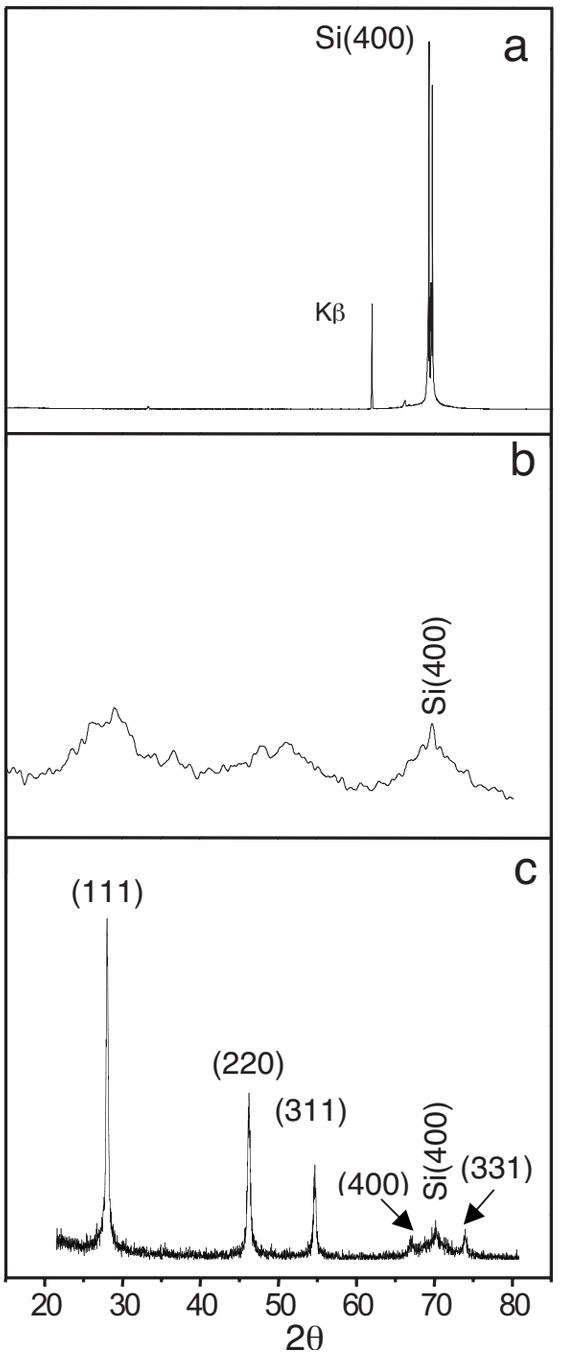

Figure 10. X-ray diffraction patterns of (a) p-doped Si(100) wafer, (b) germanium film electrodeposited on p-doped Si(100) at 100 V for 20 min, and (c) the same film after annealing in nitrogen atmosphere at 600°C. The indexed reflections in (c) are for cubic germanium.

of about 2.5 Å thick), the XPS spectrum exhibited a strong peak at ~29.5 eV, which corresponds to Ge^0 3d electrons (Fig. 9). As in the EDS spectra, XPS also shows traces of potassium cations (K^+ 3s).

The crystallinity of the films was studied by X-ray powder diffraction with Cu radiation. The clean silicon wafer (100) surface shows an intense sharp doublet at ~70°, which corresponds to the Kα1 and Kα2 diffractions of the Si(400) planes and a much weaker peak at ~62°, which is due to the Kβ diffraction of the same planes (Fig. 10a). The Si(400) peak can also be seen after the germanium film is electrodeposited but is much weaker, as can be expected (Fig. 10b). The rest of the powder pattern of the as-deposited film shows broad features at around 30 and 50° and indicates amorphous films. Similar amorphous films were obtained by Huang et al. after cathodic electroplating from $GeCl_4$ solutions. However, upon annealing of the samples, the same group observed crystallization of the films. Similar annealing of our films in flowing nitrogen gas at 400°C for 2 h showed only improved crystallinity. However, after heating at 600°C for 20 min, the films deposited at 100 V and at 3 mA/cm^2 exhibited intense sharp diffraction peaks corresponding to the (111), (220), (311), (400), and (331) reflections of elemental germanium (Fig. 10c). The samples deposited at lower current densities under the same annealing conditions did not show crystallization.

Conclusion

We have shown that germanium films can be deposited anodically at room temperature by a relatively simple electrochemical process from ethylenediamine solutions of K_4Ge_9. The resulting films are amorphous, but the thicker ones ($\geq$320 nm) become crystalline upon annealing under nitrogen. All prior work pertaining to electrodeposition of germanium on metal and semiconductor substrates concerned deposition at the cathode. Those deposition baths contained germanium halides or, in a few instances, germanium oxides[9] either as melts or dissolved in aqueous media, glycols, diols, or ionic liquids. There is a threefold advantage in using anionic Ge_9^{4-} clusters for electrodeposition. First, the current efficiencies are high as, for all practical purposes, no side reactions occur at the anode. Second, the usage of polar organic solvents such as ethylenediamine eliminates the large hydrogen overpotentials associated with aqueous media. Third, the disadvantages of high viscosities associated with nonaqueous media such as propylene glycol or the high costs pertaining to ionic liquid solvents are also circumvented.

Acknowledgments

This material is based upon the work supported by the Department of Energy, Office of Basic Energy Sciences, under award no. DE-FG02-07ER46476.

University of Notre Dame assisted in meeting the publication costs of this article.

References

1. P. V. Kamat, *J. Phys. Chem. C*, **112**, 18737 (2008).
2. D. Choi, Y. Ge, J. S. Harris, J. Cagnon, and S. Stemmer, *J. Cryst. Growth*, **310**, 4273 (2008).
3. M. I. Alonso, M. Garriga, A. Bernardi, A. R. Goni, A. F. Lopeandia, G. Garcia, J. Rodriguez Viejo, and J. L. Labar, *Thin Solid Films*, **516**, 4277 (2008).
4. Q. Wan, C. L. Lin, N. L. Zhang, W. L. Liu, G. Yang, and T. H. Wang, *Appl. Phys. Lett.*, **82**, 3162 (2003).
5. C. Bonafos, B. Colombeau, A. Altibelli, M. Carrada, G. Ben Assayag, and B. Garrido, *Nucl. Instrum. Methods Phys. Res. B*, **178**, 17 (2001).
6. S. K. Fukatsu, H. Fujita, Y. Yaguchi, Y. Shiraki, and R. Ito, *Appl. Phys. Lett.*, **59**, 2103 (1991); O. Leifeld, E. Müller, D. Grutzmacher, and K. Kern, *Thin Solid Films*, **380**, 176 (2000); T. F. Wietler, E. Bugiel, and K. R. Hofmann, *Thin Solid Films*, **517**, 272 (2008).
7. M. Zacharias and P. M. Fauchet, *J. Non-Cryst. Solids*, **227–230**, 1058 (1998).
8. G. F. Fulop and R. M. Taylor, *Annu. Rev. Mater. Sci.*, **15**, 197 (1985).
9. G. Szekely, *J. Electrochem. Soc.*, **98**, 318 (1951); W. Paatsch, *J. Electrochem. Soc.*, **124**, 1505 (1977); N. Brinda-Konopik and G. Schade, *Electrochim. Acta*, **25**, 697 (1980).
10. F. Endres and C. Schrodt, *Phys. Chem. Chem. Phys.*, **2**, 5517 (2000).
11. F. Endres, *Phys. Chem. Chem. Phys.*, **3**, 3165 (2001).
12. I. Mukhopadhyay and W. Freyland, *Chem. Phys. Lett.*, **377**, 223 (2003).
13. Q. Huang, S. W. Bedell, K. L. Saenger, M. Copel, H. Deligianni, and L. T. Romankiw, *Electrochem. Solid-State Lett.*, **10**, D124 (2007).
14. Q. Huang, H. Deligianni, and L. T. Romankiw, *Electrochem. Solid-State Lett.*, **10**, D121 (2007).
15. R. B. Taylor, A. G. Fox, J. L. Hope-Weeks, R. S. Maxwell, S. M. Kauzlarich, and W. H. Lee, *Mater. Sci. Eng., B*, **B96**, 90 (2002).
16. P. F. McMillan, J. Gryko, C. Bull, R. Arledge, A. J. Kenyon, and B. A. Cressey, *J. Solid State Chem.*, **178**, 937 (2005).

17. G. S. Armatas and M. G. Kanatzidis, *Adv. Mater.*, **20**, 546 (2008).
18. D. Sun, A. E. Riley, A. J. Cadby, E. K. Richman, S. D. Korlann, and S. H. Tolbert, *Nature (London)*, **441**, 1126 (2006).
19. A. E. Riley, S. D. Korlann, E. K. Richman, and S. H. Tolbert, *Angew. Chem., Int. Ed.*, **45**, 235 (2006).
20. T. H. Teherani, W. J. Peer, J. J. Lagowski, and A. J. Bard, *J. Electrochem. Soc.*, **125**, 1717 (1978); E. W. Brooman, *Electrodeposition and Surface Treatment*, **2**, 1 (1973).
21. A. Ugrinov and S. C. Sevov, *J. Am. Chem. Soc.*, **125**, 14059 (2003).
22. F. Endres and S. Z. El Abedin, *Phys. Chem. Chem. Phys.*, **4**, 1640 (2002).
23. M. Saitou, K. Sakae, and W. Oshikawa, *Surf. Coat. Technol.*, **162**, 101 (2003).
24. F. Liu, F. Wu, and M. G. Lagally, *Chem. Rev. (Washington, D.C.)*, **97**, 1045 (1997).
25. T. F. Fässler, H.-J. Muhr, and M. Hunziker, *Eur. J. Inorg. Chem.*, **1998**, 1433.